Journal of Applied Polymer Science

Polycarbonate-based composites reinforced by in situ polytetrafluoroethylene fibrillation: Preparation, thermal and rheological behavior

Diego Antonioli,[1] Katia Sparnacci,[1] Michele Laus,[1] Luca Boarino,[2] Maria Cristina Righetti[3]

[1]Dipartimento di Scienze e Innovazione Tecnologica (DISIT), Università del Piemonte Orientale "A. Avogadro", INSTM, UdR Alessandria 15121, Alessandria, Italy

[2]Nano Facility Piemonte, Electromagnetism Division, Istituto Nazionale di Ricerca Metrologica, Strada delle Cacce 91, Torino 10135, Italy

[3]CNR, Istituto per i processi Chimico-Fisici, UOS di Pisa 56124, Pisa, Italy

Correspondence to: M. Laus (E-mail: michele.laus@mfn.unipmn.it)

ABSTRACT: Fibrillar reinforced composites of polytetrafluoroethylene (PTFE) and polycarbonate (PC) were prepared by in situ fibrillation of PTFE into PC matrix using twin screw extruder. Different samples were obtained by varying the relative ratio between PC and PTFE. The rheological properties of the PC/PTFE composites were found to depend on concentration of the PTFE fibrils. The melt strength analysis in nonisothermal conditions was also studied. The increase in force and decrease in drawability with increasing the PTFE content are associated with the PTFE fibrils formed in situ during the thermomechanical process in twin screw extruder. © 2015 Wiley Periodicals, Inc. J. Appl. Polym. Sci. **2015**, *132*, 42401.

KEYWORDS: composites; rheology; thermal properties

Received 17 December 2014; accepted 23 April 2015
DOI: 10.1002/app.42401

INTRODUCTION

Polytetrafluoroethylene (PTFE) is a polymer commonly used as solid lubricant because of its good resistance to chemical attacks, high melting temperature, and low coefficient of friction.[1] Unfortunately, the low adhesion and the low wettability of the PTFE result in a low degree of dispersion of this polymer in other matrices, which often results in inefficient mechanical coupling with the second component of the blend. In the past years, several method to enhance the wettability and compatibility of PTFE were developed as high reactive chemicals[2,3] or high energy inputs (UV or plasma).[4–7] An alternative and promising nondestructive approach to produce compounds with a perfect dispersion of PTFE particles is based on the preparation of core-shell particles in which the core is constituted by PTFE and the shell by a conventional polymer.[8] PTFE/Polystyrene (PS),[9] PTFE/Polymethylmethacrylate (PMMA),[10,11] and PTFE/polyacrylates[12] core-shell nanoparticles and nanocomposites were prepared using seeded free emulsion polymerization. Monodispersed core–shell nanoparticles were obtained using this approach and were used to produce 2D[13] and 3D[14,15] (polymer opal) arrays. Coprecipitation techniques were also used to produce nanocomposites and microcomposites. The precipitation of preformed polymer as polyamide-imide[16] and poly(ether sulphone)[17–19] into a PTFE latex containing submicrometer size nanoparticles was recently used.

From a point technological of view, melt mixing is the most common procedure for preparation of polymeric blends, with the advantage that it does not require use of solvents. Thermodynamic miscibility of the polymeric components, which occurs if the homogeneity reaches the molecular level, is quite rare in commercial practice.[20] Blends thermodynamically not miscible are instable with respect to time and tend to separate, developing homogeneous phases with continuous phase boundary, which affects negatively the mechanical properties of the products. Although the lack of chemical interaction between the blend constituents is generally considered a disadvantage, mixtures of immiscible polymers can often create a partnership with good mechanical properties, with the majority component that constitutes the homogeneous matrix and the minority component (the reinforcement) the dispersed phase. The size and morphology of the dispersed polymer are crucial to the final physical properties of the blend and can vary tremendously depending on the couple of the polymers and the preparation method.[20] Thus, by using the correct combination of manufacturing and postprocessing conditions, it is possible to generate different reinforcement morphologies from a single immiscible blend pairing.

It was recognized that the mechanical characteristics of many polymers can be improved by means of reinforcing elements that

grow in the amorphous matrix during the manufacturing process.[21–30] Processing an incompatible polymer pair in which the dispersed phase forms in situ reinforcing fibers is a useful way to achieve good mechanical properties. Unlike traditional polymer composites, the reinforcements are not available as a separate material but are created simultaneously with the isotropic matrix.

Various self-reinforced composites have been developed and studied. Blends of flexible commercial polymers with thermotropic liquid crystalline polymers (LCP) have been prepared and characterized.[21–23] The processing of the blends at high elongation flow converts the rigid rod-like LCP domains into dispersed and high oriented microfibrils, which act as reinforcing phase. The practical utility of these systems is however quite low, as LCP are too expensive for common and general applications. Another class of microfibrillar immiscible polymer–polymer composites, known as microfibrillar reinforced composites (MFC), has been recently developed.[24–27,31] A MFC comprises an isotropic polymer matrix reinforced with microfibrils or nanofibrils of a different polymer. The fibrils, characterized by a high aspect ratio, are obtained through a mechanical process of alignment and stretching. The manufacturing of an MFC comprises three successive different steps: (i) melt blending and extrusion, (ii) cold drawing of the blend, and (iii) annealing of the drawn blend at a temperature above the melting temperature of the lower melting component, but below the melting temperature of the other component. On drawing, the components of the blends are oriented, and microfibrils of both of them are generated. During annealing, the microfibrils of the polymer with the lower melting temperature undergo fusion, whereas the microfibrils of the higher melting component are maintained, which results ultimately in an isotropic relaxed matrix with microfibrils chaotically embedded. With this procedure polypropylene/poly(ethylene terephthalate), polyethylene/poly(ethylene terephthalate), polyamide 6/poly(ethylene terephthalate), poly(butylene terephthalate)/poly(ethylene terephthalate) MFC were preparated.[24–27] Microfibrils with diameter of about 2–4 μm have been reported.[24–27] One of the advantages of the MFC is that the preparation of these composites does not require the dispersion of a preformed reinforcing material into the matrix, thus avoiding one of the biggest challenges in microcomposite and nanocomposite creation, namely agglomeration of the reinforcing phase.[28]

A further step toward a simplification in the MFC preparation can be achieved by using PTFE to generate microfibrils.[32] It is known that stable fibrils develop in PTFE samples under loading conditions to dissipate energy and stabilize a crack tip by bridging.[33–35] The irreversible formation of fibrils is an orientation process that provides a significant increase in the elastic strength of PTFE. The stability of PTFE fibrils was found primarily determined by temperature, with additional dependence on loading rate and microstructure anisotropy. The use of PTFE allows to reduce the steps for the MFC preparation from three to one, with the only extrusion process sufficient to produce a polymeric matrix enriched with PTFE microfibrils. PTFE particles can be easily fibrillated under shear or extensional flow, at the process temperature of an immiscible matrix, which results in a significant increase in the melt strength of the system.[32,36]

The aim of this contribution is to report on the preparation of fibrillar reinforced composites based on polycarbonate (PC) and PTFE. PC is a thermoplastic polymer widely used for its hardness and toughness as a single-phase material or as the matrix of a composite material.[37,38] The effect of PTFE fibrillation on thermal and rheological properties of PC/PTFE composites is here analyzed and discussed.

EXPERIMENTAL

Materials

PTFE DF680 powder (Solvay Solexis) consists a spherical particle with an average diameter of 500 μm. Polycarbonate Makrolon 2407 (PC) was provided by Bayer.

Composites Preparation

The compounding processes of composites were performed using a corotating twin-screw extruder Collin (Germany) having a screw diameter of 25 mm and a barrel length of 450 mm ($L/D = 18$). For the composites production, PC pellets and the powdery PTFE material were fed simultaneously into the hopper by gravimetric dosing. The materials had been previously dried under vacuum oven for 24 h at 120°C. The relatively low extrusion temperature was chosen to produce an high melt viscosity thus resulting in a relatively high shear stress exerted by the polymer melt toward the PTFE agglomerates (260, 290, 260, 255, and 255°C). A constant rotation speed of 70 rpm was applied during the melt mixing process. Throughout the article, label PC indicates PC samples processed in the extruder without addition of PTFE.

Composites Characterization

Morphological investigation was performed using an Inspect F SEM-FEG (scanning electron microscope-field emission gun) microscope from FEI company, with a beam diameter of 3 nm, both on the plain sample powders and on the blend fractured specimens, obtained after immersion in liquid nitrogen for 30 min. To avoid electron charging effects during SEM analysis, the samples were coated with 3 nm of gold, by means of a Cressington 108 Auto sputter coater in argon plasma atmosphere (0.15 mbar) with an emission current of 25 mA.

Differential scanning calorimetry (DSC) was carried out using a Mettler-Toledo DSC 821 apparatus. Samples of about 5 mg were used. The instrument was calibrated with high purity at 10°C min^{-1}. Dry nitrogen was used as purge gas.

Steady-state shearing and dynamic flow properties were measured by a strain-controlled rotational ARES (Rheometric Scientific) at 260°C. Frequency sweep tests were performed using a parallel plate geometry ($d = 25$ mm) over a frequency range from 100 to 0.1 rad s^{-1}. Because of the low viscosity of the PC matrix, the strain used in the frequency tests was 5.0%. The viscoelastic response was found linear from 0.01 to 10% in the strain sweep analysis. Step rate tests were carried out using a cone-plate geometry ($d = 25$ mm and a cone angle of 0.1 rad) over a shear rate range from 0.005 to 20 s^{-1}.

The shear flow studies of composites were performed using capillary a rheometer Rheo-Tester 2000 (Gottfert). A capillary die with dimensions of 0.5 mm diameter, 5.0 mm length, and 180° entry angle with an aspect ratio (L/D) of 5/0.5 was used. The

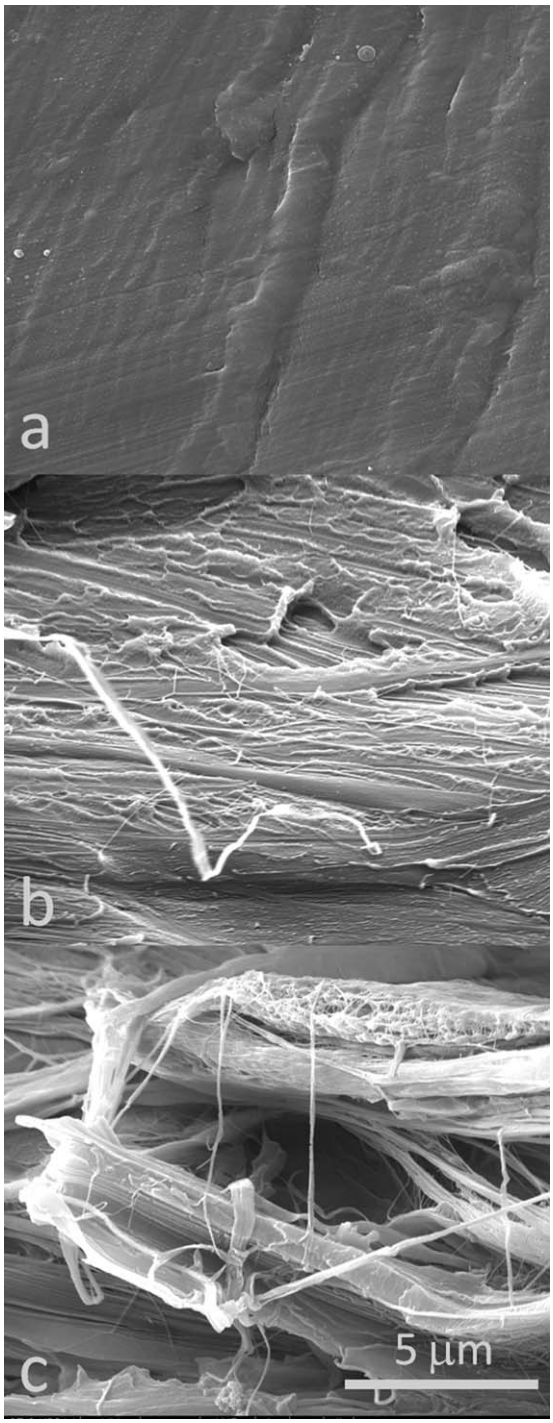

Figure 1. SEM micrographs (magnification ×12,000) of cryofractured surfaces of PC (a), PC/PTFE 1% (b), and PC/PTFE 5% (c).

test was carried out using a wide range of shear rates (20–12,000 s^{-1}) at 260°C.

Melt strength evaluations were performed using a Rheotens 71.97 (Gottfert) in a combination with single screw extruder ($D = 10$ mm and $L = 300$ mm, $L/D = 30$) at 260°C. The diameter and length of extruder die were 2 and 30 mm, respectively. The rheotens equipment was set applying wheel acceleration of 60 mm s^{-2}, and a gap between wheels of 0.4 mm. The distance between the extruder die and the rheotens wheels was 110 mm. An initial linear velocity of 50 mm s^{-1} was applied.

Dynamical mechanical analysis was performed using a dynamic mechanical analyzer Rheometric Scientific DMTA V, using the three point bending geometry. A static to dynamic stress ratio of 120% and a scanning rate of 4°C min^{-1} were chosen. The strain was sufficiently small to be within linear viscoelastic range. The samples for the dynamic-mechanical analysis were prepared introducing the sample into a rectangular mould. The entire assembly was then placed between press plates with a nominal pressure of 4.9×10^7 Pa and allowed to stand at room temperature for 20 min. The temperature was then raised to 210°C and the pressure released to 4.9×10^6 Pa. After 15 min, the sample was cooled to room temperature and recovered as rectangular 30 mm × 5 mm × 2 mm sheets.

RESULTS AND DISCUSSION

The PC/PTFE composites were prepared by melt mixing in twin screw extruder at 260°C, the temperature at which PC is generally processed. As 260°C is below the melting temperature of PTFE, formation of fluorinated polymer fibrils can be achieved. Samples containing 1 and 5 wt % of PTFE were prepared.

SEM was used to investigate the microstructure of PC/PTFE samples prepared by compression molding and cryofractured. Figure 1 shows the fractured surface micrographs of PC and its composites with PTFE. In case of PC, brittle fracture with smooth surfaces occurs. In contrast, in case of samples PC/PTFE 1% and PC/PTFE 5%, ductile fracture with significant localized deformation in the form of fibrils is observed. The fibrils are 200–300 nm in diameter and can measure several microns in length. In addition, the surface density of fibrils in case of PC/PTFE 5% is substantially higher than for PES/PTFE 1%. The present data further stress the pronounced tendency of PTFE particles toward fibrillation and indicates that individual fibers can be obtained from the cold coalescence of adjacent particles stretched. In addition, the homogeneous distribution of PTFE fibrils at the cryofractured surfaces confirms the homogeneous distribution of PTFE particles within the composites, as already proven for PTFE/PP composites.[32]

The thermal behavior of various samples was studied by DSC. The DSC first cooling and second heating curves of PC/PTFE 5%, PC/PTFE 1%, and PTFE at −10°C min^{-1} and + 10°C min^{-1}, respectively, are illustrated in Figure 2. The Figure shows also the DSC trace upon heating of neat PC, which evidences a glass transition around 140°C. The crystallization and the melting of PTFE in the plain polymer and in the composites occurs at 310°C and 326°C, respectively, in agreement with literature data.[39]

The glass transition temperature observed in the heating curves of the PC/PTFE 1% and 5% composites corresponds to that of pure PC, which means that PTFE and PC are completely immiscible polymers. It is worth noting that the PC/PTFE composites, subjected to the same thermal history as plain PC, exhibit an enthalpy recovery peak in correspondence of the glass transition, differently from plain PC. This means that the PC chains motion are modified by the presence of PTFE: the conformational rearrangements of the PC segments seem favored in

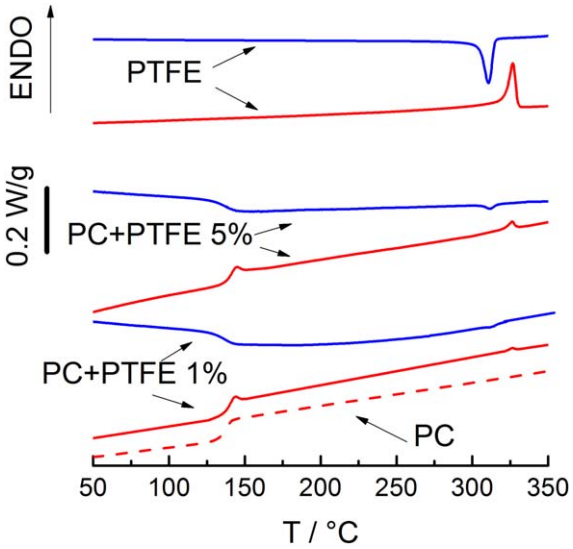

Figure 2. DSC second heating (dashed red curve) at 10°C min^{-1} for PC and DSC second heating (red curves) and first cooling (blue curves) at 10°C min^{-1} for PC/PTFE 5% and PTFE. The DSC traces for PTFE sample were divided by 5. [Color figure can be viewed in the online issue, which is available at wileyonlinelibrary.com.]

the composites, probably owing to an increased free volume, which confirms the hypothesis that PTFE and PC are noninteracting separated phases. The specific heat capacity increments at T_g, normalized to the nominal PC content, correspond, within the experimental error, to the specific heat capacity increments of pure PC, which confirms the composition of the blends.

It is well known that the melt rheological properties of a blend are very sensitive to the state of dispersion of the two components. Dynamic oscillatory shear measurements of polymeric materials are generally performed by applying a time dependent strain $\gamma(t) = \gamma_0 \sin(\omega t)$ and measuring the resultant shear stress $\sigma(t) = \gamma_0 [G' \sin(\omega t) + G'' \cos(\omega t)]$, where G' and G'' are the storage and loss moduli, respectively and ω the frequency.[40] The shear storage modulus G', the loss storage modulus G'', and the loss tangent tan δ (G''/G') of pure PC and PC/PTFE composites as a function of frequency at 260°C are shown in Figure 3.

Theory predicts that the terminal flow behavior of polymers is expressed by the law $G' \propto \omega^2$. This is satisfied by neat PC from 10^2 to about 1 rad s^{-1}. At lower frequencies, PC exhibits a plateau-like regime, typical of commercial products with a broad molecular weight distribution.[41] The addition of PTFE influences the storage and loss moduli at low frequency, which both reflect the fully relaxed polymer chain dynamics. The storage modulus increases markedly and becomes less dependent on the frequency with increasing the PTFE content. Also the loss modulus increases with the PTFE concentration, but the rate of increase is lower with respect to G′, with the result that the maximum of tan δ reduces and shifts to higher frequencies with the PTFE content.[42] The viscoelastic peak occurs at the frequency of about 0.5 rad s^{-1} for the neat PC, about 5 rad s^{-1} for PC/PTFE 1% sample, and about 15 rad s^{-1} for PC/PTFE 5% composite, showing that the material becomes progressively more elastic. According to experimental evidences collected for immiscible polymer blends, the different dependence on the PTFE content, exhibited by the G' and G'' moduli, proves that the PC matrix and the PTFE fibrils do not interact chemically.[42–44] Indeed the loss tangent tan δ is very sensitive to the structural change of materials and its progressive reduction with increasing the PTFE content can be explained as due to the presence of various structures such as PTFE agglomerations[45,46] and networks[47] (fibrils). The plateau-like regime extends from 10^0 rad s^{-1} to frequencies progressively increasing with increasing the PTFE content. This liquid-like to solid-like behavior at low frequency has been reported for other filler-thermoplastic composites and have been ascribed to increasing interactions between the filler particles or fibers, eventually leading to a formation of a interconnect PTFE fibril structure.[42,48]

The bilogarithmic plots of the complex viscosity $|\eta^*|$ versus ω $(|\eta^*| = [G'(\omega)^2 + G''(\omega)^2]^{1/2}/\omega)$, obtained by parallel plate oscillating rheometer at 260°C, and the bilogarithmic plots of the steady-state shear viscosity η versus shear rate $d\gamma/dt$, obtained by combined cone-plate rotational rheometer and capillarity rheometer at 260°C in a wide range of shear rate, shown in Figure 4(A) and (B) respectively, reveal a significant difference between plain PC and the composites, particularly at low frequency.

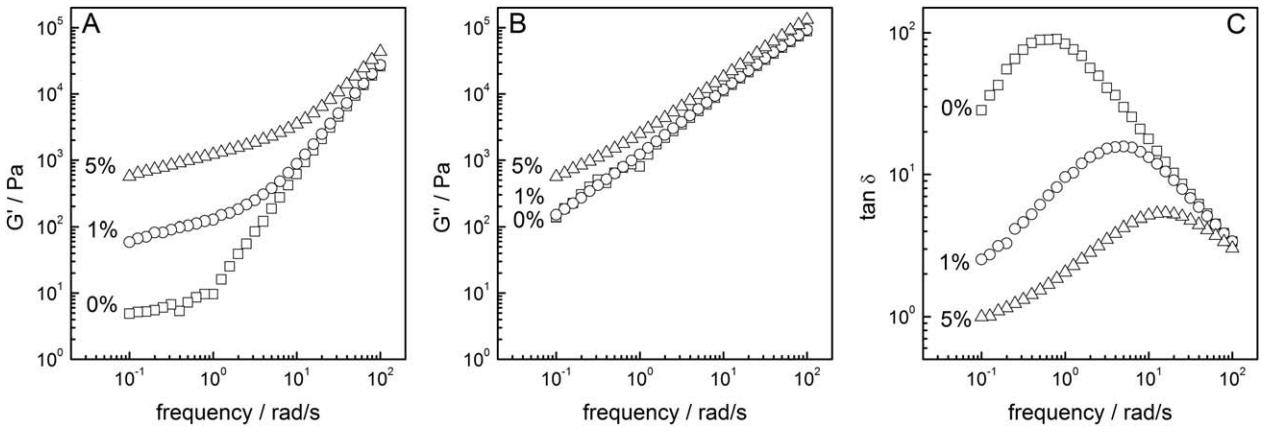

Figure 3. Trend of shear storage modulus G' (A), loss storage modulus G'' (B), and loss tangent tan δ (C) as a function of frequency at 260°C for PC (square symbols), PC/PTFE 1% (circle symbols), and PC/PTFE 5% (triangle symbols).

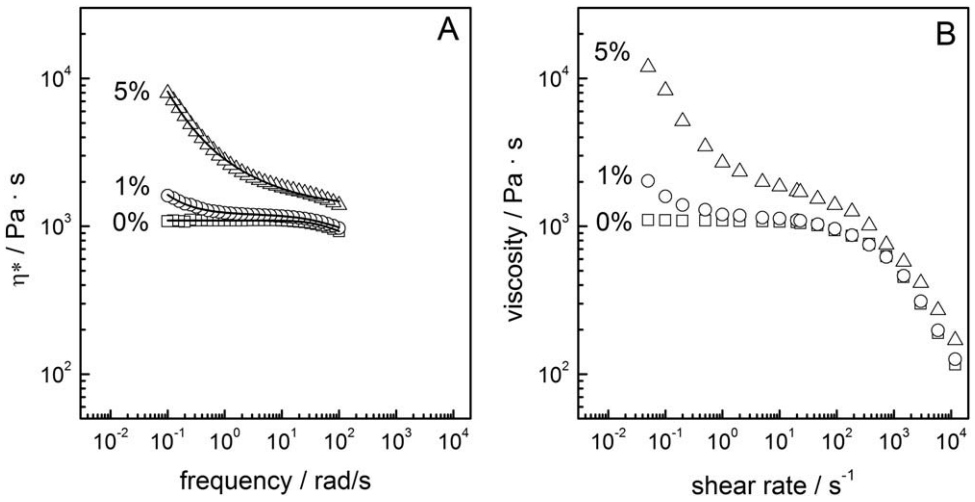

Figure 4. Trend of complex melt viscosity η^* as a function of frequency (A) and flow curve as a function of shear rate (B) at 260°C for PC (square symbols), PC/PTFE 1% (circle symbols), and PC/PTFE 5% (triangle symbols). In addition, (A) shows the Carreau–Yasuda fit for PC, PC/PTFE 1%, and PC/PTFE 5% (lines).

The complex melt viscosity increases with the PTFE content at low frequency. Newtonian plateau at low shear and shear thinning trend at high deformation are observed for the neat PC. At low shear rate an increase of viscosity is recorded for the PC/PTFE composites and particularly for the composites with PTFE amount of 5%, in agreement with dynamic flow measurement at low frequency. This is in accordance with theoretical expectations and experimental observations for fiber reinforced composites.[49–51] PC/PTFE 1% remains essentially Newtonian with modest increase of the complex viscosity only at the lowest frequency. Conversely, PC/PTFE 5% shows very strong non-Newtonian behavior, retaining a viscosity significantly greater than that of plain PC also at higher frequencies. This composite exhibits a very strong shear thinning trend. A Carreau–Yasuda model with a yield stress was used to account for the increase of viscosity at low shear rate.[52]

$$\eta*(\omega)=\frac{\sigma_0}{\omega}+\eta_0[1+(\lambda\omega)^a]^{(n-1)/a}$$

where σ_0 is the melt yield stress, η_0 is the zero shear viscosity, λ is the time constant, a is the Yasuda parameter, and n is the dimensionless power law index. For determining the parameters of the neat PC, σ_0 was set equal to 0. Subsequently, these values are used as starting parameters for fitting the complex viscosity of the PC/PTFE composites. To simplify, the power law index n of the PC/PTFE composites is assumed equal to that of the matrix.[52] The parameters used to fit the experimental data are collected in Table I. The Carreau–Yasuda fit curves of the complex viscosity, shown in Figure 4(A), demonstrate that there is a good agreement between the experimental and the calculated data. The Carreau–Yasuda parameters are found to vary with the PTFE content. The time constant λ and the parameter a do not significantly change, unlike the melt yield stress σ_0, which increases with increasing the PTFE content. This quantity controls the increase of complex viscosity at low frequency and can be put into relation with the formation of PTFE fibrils in the PC matrix.[53,54]

According to the Cox-Merz rule, the complex viscosity (from dynamic rotational rheometer) and the steady shear viscosity (from capillary rheometer) are super-imposable for numerically equivalent values of frequency ω and shear rate.[55] Pure PC and both the composites obey the rule, which means that orientation of the PTFE fibrils remains substantially unchanged during the steady state and dynamic experiment.[56]

The melt strength properties of the PC/PTFE composites and the neat PC were analyzed by a Rheotens 71.97 in a combination with single screw extruder at 260°C. Figure 5 reports the force as a function of wheel speed for composite materials and neat PC. The increase in force and the decrease in drawability with increasing the PTFE content, in agreement with the shear viscosity measurements, can be associated with the presence of PTFE fibrils formed in situ during the thermomechanical process in the twin screw extruder.[42]

The dynamic mechanical behavior of the PC/PTFE samples was also studied by DMTA using the three point bending geometry in the linear viscoelasticity region at the frequency of 1 Hz, between −140°C and the temperature at which the samples lost their dimensional stability, with a heating rate of 4°C min^{-1}. Figure 6 illustrates the trends of the storage modulus E' and of tan δ as a function of temperature. The E' curves displays a marked drop at about 150°C, which corresponds to the glass transition of PC, and a intense step in correspondence of the β secondary relaxation located in the range $-100 < T < -50$°C. The good impact resistance of PC has always been attributed to secondary relaxation originating from local movement within the chains.[40] Some authors found that the broad β relaxation may be resolved into more than

Table I. Parameters Used in the Carreau–Yasuda Model with Yield Stress for PC/PTFE Composites

Sample	σ_0 (Pa)	η_0 (Pa s)	λ	A	n
PC	0	1095	0.027	2.12	0.84
PC/PTFE 1%	44	1196	0.029	1.28	0.84
PC/PTFE 5%	482	1377	0.036	0.75	0.84

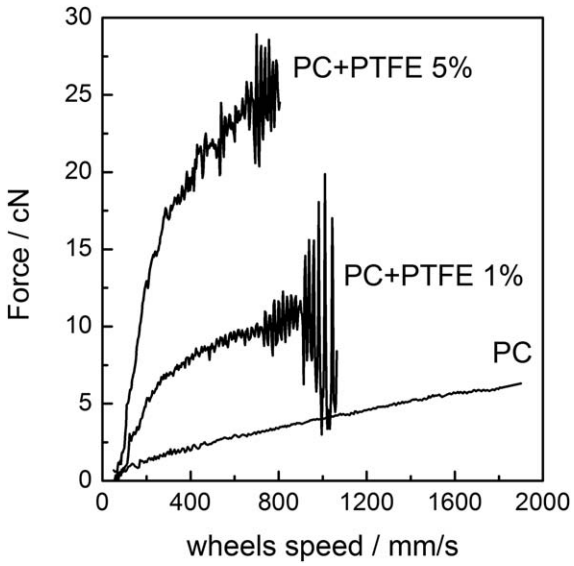

Figure 5. Melt strength as a function of drawdown velocity (relative drawdown velocity) for PC, PC/PTFE 1%, and PC/PTFE 5%.

one process,[57,58] while others did not show evidence of an existing structure within the relaxation.[59]

The β relaxation has been associated with the local motions of both the strongly dipolar carbonate groups and the phenyl groups.[58] The position and the width of the glass transition do not change in the presence of PTFE, which confirms the absence of interfacial interactions between the two components.[40] The addition of PTFE increases the stiffness of the composite, as below the glass transition temperature of polycarbonate, the storage modulus E' increases with the PTFE amount, as already proven for PTFE/PP composites.[32] The effect is much more marked with reducing the temperature. At room temperature, the storage modulus E' value for PC is 900 MPa, for PC/PTFE 1% sample is 950 MPa, and for PC/PTFE 5% is

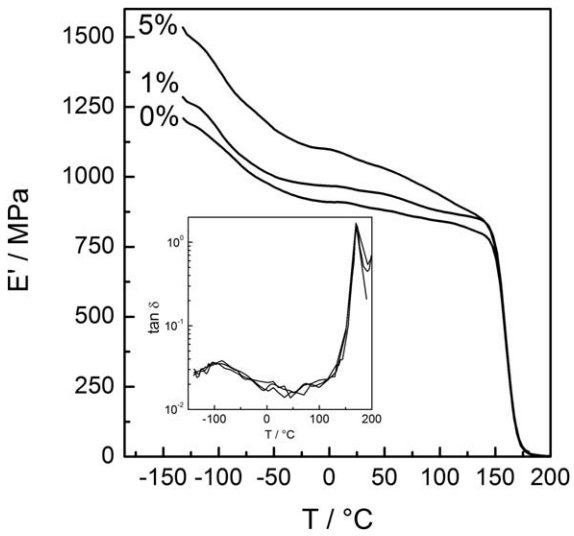

Figure 6. Trend of dynamic storage modulus E' as a function of temperature for PC, PC/PTFE 1%, and PC/PTFE 5%. In the inset the tan δ curves are reported.

1050 Pa. Similar behavior were obtained for PTFE-based nanocomposites obtained from core–shell nanoparticles,[60,61] coprecipitation of technopolymers and PTFE,[18] and in situ PTFE fibrillation during compounding with polypropylene.[32]

Also the β secondary motions are not affected by the PTFE fibers, as evidenced by both the approximately constant E' decrease at about −100°C, and, more distinctly, by the corresponding tan δ peak, which results independent of the PTFE content. This confirms that localized interactions do not develop between the PTFE fibers and the PC segments that give rise to the β relaxation.

CONCLUSIONS

The effect of crystalline PTFE microfibrils on the mechanical, rheological, and thermal properties of PC was investigated and discussed. The absence of specific interactions in the composites at the interface PC/PTFE was proven by the constancy of the glass transition temperature, which was found to correspond to the T_g of plain PC. Despite that PTFE and PC are completely immiscible, the mechanical properties of the microfibrillar composites PC/PTFE turned out improved, owing to reinforcement action exerted on the PC matrix by the PTFE microfibrils. The presence of PTFE microfibrils produces also a progressive increase in viscosity and in melt strength and a reduction in drawability with increasing the PTFE content.

In conclusion, the use of PTFE to generate microfibrils is a favorable strategy to expedite the preparation of microfibrillar reinforced composites, reducing the preparation steps to only the extrusion process. The resultant mechanical properties are those characteristic of a reinforced material.

REFERENCES

1. Tsibouklis, J.; Nevell, T. G. *Adv. Mater.* **2003**, *15*, 647.
2. Zhao, B.; Brittain, W. J.; Vogler, E. A. *Macromolecules* **1999**, *32*, 796.
3. Ji, L. Y.; Kang, E. T.; Neoh, K. G.; Ridge, K.; Tan, K. L. *Langmuir* **2002**, *18*, 9035.
4. Akinay, E.; Tincer, T. *J. Appl. Polym. Sci.* **2001**, *79*, 816.
5. Konig, U.; Nitschke, M.; Menning, A.; Eberth, G.; Pilz, M.; Arnhold, C.; Simon, F.; Adam, G.; Werner, C. *Colloids Surfaces B Bionterfaces* **2002**, *24*, 63.
6. Pompe, G.; Häußler, L.; Pötschke, P.; Voigt, D.; Janke, A.; Geißler, U.; Hupfer, B.; Reinhardt, G.; Lehmann, D. *J. Appl. Polym. Sci.* **2005**, *98*, 1308.
7. Pompe, G.; Häußler, L.; Adam, G.; Eichhorn, K.-J.; Janke, A.; Hupfer, B.; Lehmann, D. *J. Appl. Polym. Sci.* **2005**, *98*, 1317.
8. Sparnacci, K.; Antonioli, D.; Deregibus, S.; Laus, M.; Zuccheri, G.; Boarino, L.; De Leo, N.; Comoretto, D. *J. Nanomater.* **2012**, *2012*, 980541.
9. Giani, E.; Sparnacci, K.; Laus, M.; Palamone, G.; Kapeliouchko, V.; Arcella, V. *Macromolecules* **2003**, *36*, 4360.

10. Kapeliouchko, V.; Palamone, G.; Poggio, T.; Zuccheri, G.; Passeri, R.; Sparnacci, K.; Antonioli, D.; Deregibus, S.; Laus, M. *J. Polym. Sci. Part A Polym. Chem.* **2009**, *47*, 2928.
11. Laus, M.; Sparnacci, K.; Antonioli, D.; Deregibus, S.; Kapeliouchko, V.; Palamone, G.; Poggio, T.; Zuccheri, G.; Passeri, R. *J. Polym. Sci. Part B Polym. Phys.* **2010**, *48*, 548.
12. Sparnacci, K.; Antonioli, D.; Deregibus, S.; Laus, M.; Poggio, T.; Kapeliouchko, V.; Palamone, G.; Zuccheri, G.; Passeri, R. *Macromolecules* **2009**, *42*, 3518.
13. Sparnacci, K.; Antonioli, D.; Deregibus, S.; Panzarasa, G.; Laus, M.; De Leo, N.; Boarino, L.; Kapeliouchko, V.; Poggio, T. *Polym. Adv. Technol.* **2012**, *23*, 558.
14. Antonioli, D.; Deregibus, S.; Panzarasa, G.; Sparnacci, K.; Laus, M.; Berti, L.; Frezza, L.; Gambini, M.; Boarino, L.; Enrico, E.; Comoretto, D. *Polym. Int.* **2012**, *61*, 1294.
15. Sparnacci, K.; Antonioli, D.; Laus, M.; Zuccheri, G.; Boarino, L.; De Leo, N.; Comoretto, D. *AIP Conf. Proc.* **2012**, *1459*, 61.
16. Antonioli, D.; Sparnacci, K.; Laus, M.; Boarino, L.; Righetti, M. C. *Polym. Compos.* **2013**, *34*, 1451.
17. Antonioli, D.; Laus, M.; Sparnacci, K.; Deregibus, S.; Kapeliouchko, V.; Poggio, T.; Zuccheri, G.; Passeri, R.; Boarino, L. *Macromol. Symp.* **2012**, *311*, 70.
18. Righetti, M. C.; Boggioni, A.; Laus, M.; Antonioli, D.; Sparnacci, K.; Boarino, L. *J. Appl. Polym. Sci.* **2013**, *130*, 3624.
19. Righetti, M. C.; Boggioni, A.; Laus, M.; Antonioli, D.; Sparnacci, K.; Enrico, E.; Boarino, L. *Thermochim. Acta* **2013**, *571*, 53.
20. Utracki, L. A. Polymer Alloys and Blends; Hanser Gardner Publications:Cincinnati, OH, **1990**.
21. Tjong, S. C.; Liu, S. L.; Li, R. K. Y. *J. Mater. Sci.* **1995**, *30*, 353.
22. Kim, S. H.; Park, S. W.; Gil, E. S. *J. Appl. Polym. Sci.* **1998**, *67*, 1383.
23. Machiels, A. G. C.; Van Dam, J.; Posthuma De Boer, A.; Norder, B. *Polym. Eng. Sci.* **1997**, *37*, 1512.
24. Fakirov, S.; Evstatiev, M.; Petrovich, S. *Macromolecules* **1993**, *26*, 5219.
25. Evstatiev, M.; Schultz, J. M.; Petrovich, S.; Georgiev, G.; Fakirov, S.; Friedrich, K. *J. Appl. Polym. Sci.* **1998**, *67*, 723.
26. Friedrich, K.; Ueda, E.; Kamo, H.; Evstatiev, M.; Krasteva, B.; Fakirov, S. *J. Mater. Sci.* **2002**, *37*, 4299.
27. Friedrich, K.; Evstatiev, M.; Fakirov, S.; Evstatiev, O.; Ishii, M.; Harrass, M. *Compos. Sci. Technol.* **2005**, *65*, 107.
28. Shields, R. J.; Bhattacharyya, D.; Fakirov, S. *J. Mater. Sci.* **2008**, *43*, 6758.
29. An, F.-Z.; Wang, Z. W.; Hu, J.; Gao, X. Q.; Shen, K.-Z.; Deng, C. *Macromol. Mater. Eng.* **2014**, *299*, 400.
30. Fakirov, S.; Bhattacharyya, D.; Panamoottil, S. M. *Int. J. Polym. Mater.* **2014**, *63*, 777.
31. Cailiao, G.; Gongcheng, K. Y. *Polym. Mater. Sci. Eng.* **2014**, *30*, 95.
32. Jurczuk, K.; Galeski, A.; Piorkowska, E. *Polymer* **2013**, *54*, 4617.
33. Ariawan, A. B.; Ebnesajjad, S.; Hatzikiriakos, S. G.; Fluoroproducts, D. *Polym. Eng. Sci.* **2002**, *42*, 1247.
34. Brown, E. N.; Dattelbaum, D. M. *Polymer* **2005**, *46*, 3056.
35. Chen, B.; Wang, J.; Yan, F. *Tribol. Lett.* **2011**, *45*, 387.
36. Wang, K.; Wu, F.; Zhai, W.; Zheng, W. *J. Appl. Polym. Sci.* **2013**, *129*, 2253.
37. Chen, P.; Chen, J.; Zhang, B.; Zhang, J.; He, J. *J. Polym. Sci. Part B Polym. Phys.* **2006**, *44*, 1020.
38. Alves, N. M.; Mano, J. F.; Ribelles, J. L. G. *Macromol. Symp.* **1999**, *148*, 437.
39. Wang, X. Q.; Chen, D. R.; Han, J. C.; Du, Y. D. *J. Appl. Polym. Sci.* **2002**, *83*, 990.
40. Nielsen, L. E. Mechanical Properties of Polymers and Composites; Marcel Dekker: New York, NY, **1974**.
41. Pötschke, P.; Abdel-Goad, M.; Alig, I.; Dudkin, S.; Lellinger, D. *Polymer* **2004**, *45*, 8863.
42. Jurczuk, K.; Galeski, A.; Piorkowska, E. *J. Rheol.* **2014**, *58*, 589.
43. Han, C. D.; Chuang, H.-C. *J. Appl. Polym. Sci.* **1985**, *30*, 4431.
44. Han, C. D.; Yang, H. H. *J. Appl. Polym. Sci.* **1987**, *33*, 1199.
45. Zheng, Q.; Du, M.; Yang, B.; Wu, G. *Polymer* **2001**, *42*, 5743.
46. Wu, G.; Zheng, Q. *J. Polym. Sci. Part B Polym. Phys.* **2004**, *42*, 1199.
47. Hu, G.; Zhao, C.; Zhang, S.; Yang, M.; Wang, Z. *Polymer* **2006**, *47*, 480.
48. Potschke, P.; Fornes, T. D.; Paul, D. R. *Polymer* **2002**, *43*, 3247.
49. Mutel, A. T.; Kamal, M. R. In Two Phase Polymer Systems; Utracki, L. A., Ed.; Munich Carl Hanser: Munich, Germany, **1991**, p 305.
50. Kitano, T.; Kataoka, T. *Rheol. Acta* **1980**, *19*, 753.
51. Kitano, T.; Kataoka, T.; Nagatsuka, Y. *Rheol. Acta* **1984**, *23*, 20.
52. Berzin, F.; Vergnes, B.; Delamare, L. *J. Appl. Polym. Sci.* **2001**, *80*, 1243.
53. Lertwimolnun, W.; Vergnes, B. *Polym. Eng. Sci.* **2006**, *46*, 314.
54. Lertwimolnun, W.; Vergnes, B. *Polymer* **2005**, *46*, 3462.
55. Cox, W. P.; Merz, E. H. *J. Polym. Sci.* **1958**, *118*, 619.
56. Bangarusampath, D. S.; Ruckdäschel, H.; Altstädt, V.; Sandler, J. K. W.; Garray, D.; Shaffer, M. S. P. *Polymer* **2009**, *50*, 5803.
57. Watts, D. C. *Polymer* **1978**, *19*, 248.
58. Delbreilh, L.; Bernès, A.; Lacabanne, C. *Int. J. Polym. Anal. Charact.* **2005**, *10*, 41.
59. Shelby, M. D.; Hill, A. J.; Burgar, M. I.; Wilkes, G. L. *J. Polym. Sci. Part B Polym. Phys.* **2001**, *39*, 32.
60. Antonioli, D.; Laus, M.; Sparnacci, K.; Deregibus, S.; Kapeliouchko, V.; Palamone, G.; Poggio, T.; Zuccheri, G.; Passeri, R. *Macromol. Symp.* **2010**, *296*, 197.
61. Antonioli, D.; Laus, M.; Zuccheri, G.; Kapeliouchko, V.; Righetti, M. C.; Boarino, L.; Sparnacci, K. *J. Nanotechnol.* **2012**, *2012*, 875815.